Displacement mitigation mechanism and parameters sensitivity analysis of steel moment frame retrofitted by self-centering braces

Xiao Lu (xiaolu@bjtu.edu.cn)
Beijing Jiaotong University https://orcid.org/0000-0003-1395-7701
Longhe Xu
Beijing Jiaotong University

Research Article

Keywords: Steel moment frame, self-centering brace, single degree of freedom, seismic displacement mitigation, seismic resilience

Posted Date: April 5th, 2022

DOI: https://doi.org/10.21203/rs.3.rs-1514033/v1

Abstract

The steel moment frame (SMF) designed according to modern codes can prevent collapse and protect life safety, but may still experience excessive damage and residual displacement, resulting in high repair costs and long recovery time. The self-centering brace (SCB) is one of the most efficiency components to reduce the story drift and residual displacement of SMF. Although the mechanism of SCB reducing residual displacement has been fully studied, the mechanism of reducing story drift has not been well explained. Based on the equivalent single degree of freedom (SDOF) model, 24 analysis models of SMF, SMF retrofit by buckling restrained brace (BRBF), and SMF retrofit by self-centering brace (SCBF) with different fundamental periods are established in this paper. The seismic displacement mitigation mechanism of SCB is first comparatively studied using nonlinear time history analysis. Following this, 176 equivalent SDOF models representing a series of SCBFs with different key parameters (initial stiffness, post-activation stiffness coefficient and activation strength of SCB system) are established, and the influence of the key parameters of SCB on seismic responses of SCBF is discussed. Reasonable parameter value ranges are then proposed. Results show that the self-centering capacity of SCB can not only successfully reduce the residual displacement of the structure, but also effectively reduce the maximum displacement. The optimal value of the initial stiffness of the SCB is 0.6 ~ 1.2 times the initial stiffness of the SMF, the post-activation stiffness coefficient of the SCB should not exceed 0.1, and the optimal value of the activation strength of the SCB is 0.6 ~ 1.2 times the yield strength of the SMF.

1. Introduction

Steel braced frame (SMF) is widely used as a lateral force resisting system in seismic zones due to the characteristics of large initial stiffness and high ductility. Traditional steel braces are prone to buckling under compression, and the strength and stiffness are sharply degraded, thus they are unable to fully exhibit the seismic performance of the structural system. The buckling restrained brace (BRB) can yield both in tension and compression, and provides greater energy dissipation capacity and ductility to effectively reduce the displacement response of the frame and improve seismic performance. However, Erochko et al. (2011) point out that the buckling restrained braced frame experiences significant residual story drift ratio under design-based earthquake, with values between 0.8 ~ 2.0%. McCormick et al. (2008) also suggest that if the residual story drift ratio of the structure exceeds 0.5%, it is not worth repairing for the higher repair cost than the rebuild cost. And if the residual story drift ratio is close to 1%, the residents may even feel dizzy and sick. Therefore, many structures with large residual displacements after earthquakes have to be demolished and rebuilt, causing significant economic loss. As the self-centering brace (SCB) can significantly reduce the residual displacement of components and structures, it has become a popular research topic in the field of seismic engineering in recent years. For example, Christopoulos et al. (2008) developed a new self-centering energy dissipative steel brace, comprising of traditional steel brace, pre-tensioned tendons and friction damper. Miller et al. (2012) integrated the pre-tensioned superelastic nickel-titanium shape memory alloy rods into a buckling-restrained brace and then proposed a new self-centering buckling-restrained brace. Xu el al. (2017, 2022) proposed a SCB consisting of disc springs, friction devices and tubes, and comprehensively studied its hysteretic performance by cyclic tests and numerical simulations. Lin et al. (2022) proposed an improved SCB with friction and viscoelastic dampers to reduce the residual displacements and acceleration of the frames.

BRB is a widely used seismic displacement mitigation component to retrofit SMF and its displacement mitigation mechanism has been well studied. Therefore, the research on SCB is always conducted with the comparison of

BRB. As we known, the seismic displacement mitigation mechanism of BRB arises from two main aspects. The first is the increase of the initial lateral stiffness of the structure. The greater the stiffness, the smaller the displacement response of the structure. The second is the provided additional hysteresis energy dissipation. The more the additional hysteresis energy dissipated, the smaller the structural seismic responses. If the backbone curve parameters of BRB and SCB are similar, the energy dissipation capacity (the area of the hysteresis curve) of SCB is significantly smaller than that of BRB. According to these two aspects, SCB seems to have worse displacement reduction performance than that of BRB in theory. However, as noted in the literature, in addition to significantly reducing the residual displacement of the frame, the maximum instantaneous displacement of the structure reduced by SCB is comparable to or even greater than that of the BRB. Tremblay et al. (2008) examined the seismic response of 2-, 4-, 8-, 12-, and 16-story steel frames braced with SCB and BRB. The results illustrate that the maximum and residual story drift ratio experienced by steel frames with SCB are smaller than that of steel frames with BRB. Zhu and Zhang (2008) conducts comparative study on the seismic performance of 3-story and 6-story self-centering braced frames and buckling restrained braced frames using nonlinear time history analysis (NTHA). The results indicate that for the 3-story structure, the average peak story drift ratio of self-centering braced frame is slightly larger than that of buckling restrained brace for the design-based earthquake. In contrast, for the 6-story structure, the average peak story drift ratio of self-centering braced frame is slightly smaller than that of buckling restrained braced frames. Xiao et al. (2019) examined the seismic behaviors of a RC frame-tube building braced with SCB and BRB. The results show that the story drift ratio of the two systems is similar, and the peak story drift ratio of BRB system is slightly lower than that of the SCB system. It can be observed that the seismic displacement mechanism of SCB is not completely consistent with BRB, and further research is required. Moreover, the current research on SCB is mainly focused on experimental research (Christopoulos et al. 2008; Miller et al. 2012; Xu et al. 2017a, 2022), hysteresis model research (Wang et al. 2017; Xu et al. 2017b) and the typical case study (Tremblay et al. 2008; Zhu and Zhang 2008; Xiao et al. 2019). Few literatures have been reported on the influence of key parameters of SCB on the structural seismic performance from the structural system level and the reasonable key parameter values of the SCB.

Therefore, this paper will focus on the seismic displacement mitigation mechanism of SCB and the influence of the key parameters of SCB on the seismic responses of SMF retrofit by SCB (SCBF). 24 equivalent single degree of freedom (SDOF) models of SMF, SMF retrofit by BRB (BRBF) and SCBF with different fundamental periods are established. NTHA is conducted using 22 far-field earthquake ground motion records and the displacement mitigation mechanism of the SCBF is revealed through comparative study. Additionally, 176 equivalent SDOF models representing a series of SCBFs with different key parameters (initial stiffness, post-activation stiffness coefficient, activation strength) are established, and the influences of key parameters on structural displacement, acceleration, residual displacement and damage are discussed, providing a reference for the optimized design of SCBF.

2. Development Of The Equivalent Sdof System

While the refined finite element model can accurately predict the seismic response of the structure, too many variables are present in the model, and the modeling and calculation workload is large. Such aspects are not favorable for parameter analysis at the structural system level. It is widely known that an SDOF system can well predict the seismic responses of the structures whose lateral deformation dominated by the first vibration mode (Zarrin et al. 2021). For example, Christopoulos et al. (2002) used the SDOF model to study the seismic response of self-centering structures; Zhou et al. (2019) also adopted the SDOF model to study the plastic energy demand

of the self-centering structure. Therefore, this paper will establish different equivalent SDOF models to simulate the seismic response of SMFs, SCBFs and BRBFs. It is worth noting that in order to make the analysis comparable, the arrangement of the BRB and the SCB is identical in this work.

For SMF, the hysteretic behavior of the equivalent SDOF model can be simulated by a bilinear plastic model (Pirooz et al. 2021); for BRBF, the structure is considered to be composed of a SMF and BRB system in parallel, and the hysteretic property of the BRB system can be simulated by Menegotto-Pinto model (Velasco et al. 2022). The simulation method of the SCBF is similar to that of BRBF, in which the hysteretic behavior of the SCB system can be simulated by the flag shape hysteresis model (Christopoulos et al. 2002). The hysteresis models of the three structural systems are shown in Fig. 1.

As the SMF has good ductility, according to the Table 12.2-1 in ASCE 7–10, the response modification coefficient R of SMF is taken as 8, so that the yield strength F_y of the equivalent SDOF of SMF can be determined according to Eq. 1.

$$F_y = m \cdot S_a(T_1) \,/\, R \quad (1)$$

Where, m is the total seismic weight and $S_a(T_1)$ is the elastic spectral acceleration at the fundamental period of the structure. The post-yielding stiffness of SMF is taken as 1% of K_0, the initial stiffness of the equivalent SDOF of SMF. It is preliminarily assumed that the initial stiffness and strength of the bracing system used for retrofit are equivalent to those of the SMF, that is $K_{BRB} = K_{SCB} = K_0$ and $F_{y,BRB}$ $F_{a,SCB} = F_y$. Although these values may not be optimal, they can still be used as typical cases to explain the displacement mitigation mechanism of SCB. The sensitivity analysis of these key parameters will also be carried out in Section 5. In addition, the energy dissipation coefficient β of the flag shape hysteresis model is set as 1.0, which means that the SCB has maximum energy dissipation capacity under the premise of completely returning back to its initial position.

3. Ground Motion Selection

Because of the high randomness of earthquakes, the selection of different ground motion records will have a dramatic impact on the structural seismic responses predicted by the NTHA. To minimize the dispersion caused by the ground motion randomness, 22 far-field ground motion records recommended by FEMA P695 (2009) are used to conduct the NTHA in this paper. The details of these ground motion records can be seen in Appendix A in FEMA P695 (2009). It also indicates that normalizing the ground motion records by peak ground velocity can effectively mitigate the randomness but maintain the inherent variability of earthquakes for predicting structural seismic responses. Thus the normalization factors suggested by FEMA P695 are used to normalize the 22 far-field ground motion records for NTHA in this paper. The mean spectrum and individual spectrum of the normalized far-field records are shown in Fig. 2 in log format. The mean response spectrum will be used as the design target spectrum to calculate the yield strength F_y of the SMF according to Eq. 1.

4. Displacement Mitigation Mechanism Of Scb

To increase the applicability of the analysis results, 8 different initial periods T_0 = [0.2, 0.4, 0.6, 0.8, 1.0, 2.0, 3.0, 4.0] are set for the equivalent SDOF models, representing a series of SMFs from low-rise to high-rise buildings. Based on the equivalent SDOF models of the SMF, the equivalent SDOF models of SMF retrofit by BRB and SCB

are further established according to the definition in Section 2. Finally, 24 equivalent SDOF models were established. Each model uses 22 far-field ground motion records as the seismic input, and a total of 528 NTHA are conducted. In the analysis, classic Rayleigh damping is used with a damping ratio of 5%. In the subsequent discussion, the mean response results of the 22 ground motion records, including displacement, absolute acceleration and residual displacement, will be discussed.

The maximum displacement responses of the SMF, BRBF and SCBF are shown in Fig. 3a. Both the BRB and the SCB can effectively reduce the displacement response of the SMF, but as the fundamental period of the SMF increases, the reduction efficiency of displacement gradually decreases. The SCB has a slightly better displacement mitigation effect than that of the BRB, especially when the fundamental period of the SMF is longer than 1 s. The maximum acceleration responses of the SMF, BRBF and SCBF are shown in Fig. 3b. It can be observed that both the BRB and the SCB amplify the acceleration response of the steel frame, but as the fundamental period of the SMF becomes longer, the amplification effect of acceleration gradually decreases. The BRB and the SCB have the similar effect on the amplification of the steel frame acceleration. The residual displacement responses of the SMF, BRBF and SCBF are shown in Fig. 3c. As the fundamental period of the SMF extends, the residual displacement shows an increasing trend. The SCB can significantly reduce the residual displacement of the SMF and the maximum residual displacement of the SCBF is only 8% of the residual displacement of the SMF, while the residual displacement of the BRBF is similar to that of the SMF, indicating that the BRB cannot effectively reduce the residual displacement of the structure. In general, compared with BRB, the SCB can effectively reduce the residual displacement of the structure while retaining a displacement mitigation effect that is comparable to or even better than the BRB.

It is widely reported that the seismic displacement mitigation effect of BRB is predominantly due to the increase of the initial lateral stiffness and the structural hysteresis energy dissipation. For the BRB and the SCB system used for retrofit, the initial stiffness of the two systems are the same, and therefore, the initial stiffness of BRB and SCB has a completely uniform effect on displacement reduction. On the other hand, Fig. 3d indicates that the dissipated energy of BRB system is larger than that of SCB system. This means that the displacement reduced by BRB should be greater than SCB, which is clearly contradictory to findings illustrated in Fig. 3a. This phenomenon reveals that in addition to the initial stiffness and energy dissipation, there are other factors contributing to the reduction the structural displacement for SCB.

To explore the seismic displacement mechanism of SCB, it is assumed that the SCB system has no energy dissipation capability, that is, $\beta = 0$, and the maximum displacement response of the new SCBF ($\beta = 0$) is displayed in Fig. 4. Even if the SCB system has no energy dissipation capability, the displacement response of the structure can be effectively reduced, though the displacement reduction is slightly worse than that of the BRB. Figure 5 shows the detailed displacement responses of the BRBF and SCBF ($\beta = 0$) under 22 ground motions when the fundamental period of SMF is 1 s. The horizontal axis denotes the displacement response of the BRBF, the vertical axis denotes the displacement response of the SCBF with $\beta = 0$, and the diagonal line indicates that the displacement responses of the two are equal. The scatters above the diagonal demonstrate that the displacement response of the SCBF is greater than the BRBF. Conversely, the scatters below the diagonal indicate that the displacement response of the SCBF is smaller than the BRBF and 10 scatters can be observed to remain below the diagonal.

Taking the typical ground motion LANDERS_CLW-LN as an example, the displacement time history of the BRBF and the SCBF ($\beta = 0$) is shown in Fig. 6. It reveals that when the seismic force is smaller than the yield strength of the structure, the displacement responses of BRBF and SCBF are basically the same, and when the structure yields, the vibration amplitude of BRBF is smaller than the SCBF due to the strong energy dissipation capacity of the BRB. With a further increase of seismic force, the BRBF begins to generate significant residual deformation at the time of $t = 15$s. Because of the self-centering capacity of SCB, the SCBF has no obvious residual deformation, and the whole structure vibrates near the initial position. The maximum vibration amplitude of the SCBF structure occurs at 20.11 s, with the value of 49.31 mm. The maximum displacement of BRBF occurs at 21.52 s, and the maximum displacement is approximately the sum of the residual displacement (53.07 mm) and vibration amplitude (26.13 mm) at this moment. That is 79.20 mm. It can be seen that under the ground motion LANDERS_CLW-LN, although the vibration amplitude of SCBF is larger than that of BRBF, SCBF has little residual displacement, so that the maximum displacement of SCBF remains smaller than that of BRBF. This finding reveals that the self-centering capability of SCB is another factor for reducing the structural displacement response.

The vibration amplitude and residual displacement of BRBF and SCBF ($\beta = 0$) at the moment that the maximum displacement occurred under the 22 far-field ground motion records are listed in Table 1. Where "-" indicates the negative direction of vibration. The vibration amplitude of the SCBF ($\beta = 0$) is always larger than that of the BRBF due to less hysteretic energy dissipation. However, the vibration of BRBF deviates from the initial equilibrium position, leading to the significant residual displacement. The maximum displacement of BRBF is the sum of vibration amplitude and residual displacement, while the residual displacement of SCBF is negligible, and the maximum displacement is dominated by the vibration amplitude. Therefore, the total displacement response of SCBF ($\beta = 0$) is comparable to that of BRBF, and even smaller under some ground motion records. It means that ensuring that the vibration does not deviate from the initial equilibrium position is another reason for the SCB to reduce the structural displacement responses.

Table 1
Vibration amplitude and residual displacement of SCBF($\beta = 0$) and BRBF (period of SMF equals to 1.0s)

No.	Ground motion name	SCBF with $\beta = 0$		BRBF			
		time (s)	amplitude (mm)	time (s)	amplitude (mm)	residual displacement (mm)	total displacement (mm)
1	CAPEMEND_RIO270	6	125.30	6	53.06	36.65	89.71
2	CHICHI_CHY101-E	38.145	35.36	41.31	16.19	25.25	41.44
3	CHICHI_TCU045-E	45.495	-58.28	47.725	-34.41	-60.36	-94.77
4	DUZCE_BOL000	10.02	-105.40	10.01	-63.38	-22.45	-85.83
5	FRIULI_A-TMZ000	4.24	-76.13	5.765	-38.85	-8.11	-46.96
6	HECTOR_HEC000	7	83.30	6.93	60.65	20.77	81.42
7	IMPVALL_H-DLT262	32.3	60.26	8.58	57.15	26.80	83.95
8	IMPVALL_H-E11140	9.365	-106.50	8.42	46.66	11.00	57.66
9	KOBE_NIS000	10.69	91.17	7.25	-46.49	-13.28	-59.77
10	KOBE_SHI000	12.5	79.35	12.5	64.87	5.08	69.95
11	KOCAELI_ARC000	17.545	32.41	17.53	19.55	4.03	23.58
12	KOCAELI_DZC180	16.135	-47.77	9.56	27.46	22.42	49.88
13	LANDERS_CLW-LN	20.11	49.31	21.5175	26.13	53.07	79.20
14	LANDERS_YER270	16.84	179.30	17.84	66.45	80.75	147.20
15	LOMAP_CAP000	9.025	161.90	8.99	-103.62	-42.78	-146.40
16	LOMAP_G03000	4.98	44.53	10.64	18.08	52.85	70.93
17	MANJIL_ABBAR–L	12.06	-53.03	12.06	-35.80	-26.86	-62.66
18	NORTHR_LOS000	7.25	-105.90	6.88	-70.53	-47.07	-117.60
19	NORTHR_MUL009	9.02	124.30	8.37	-66.24	-14.34	-80.58
20	SFERN_PEL090	7.58	-132.50	7.62	-104.00	-59.90	-163.90
21	SUPERST_B-ICC000	13.455	116.30	13.45	56.26	43.71	99.97
22	SUPERST_B-POE270	7.67	69.93	13.58	40.95	36.73	77.68

To further demonstrate this conclusion, it is assumed that the SMF is completely elastic, meanings that the structure has no residual deformation. The SDOF model of the SMF is set to elasticity, and the hysteresis parameters of the SDOF models of BRB and SCB remain unchanged. The displacement responses of the new obtained BRBFs and SCBFs at different fundamental periods are shown in Fig. 7, in which BRB displays superior displacement response reduction than that of SCB at the fundamental period ranging from 0.2s to 4.0s. This is

because BRB and SCB have the same initial stiffness, but the energy dissipation of BRB system is better than that of the SCB system, so the vibration amplitude of BRBF is smaller than that of the SCBF. And the original SMF is elastic and has no residual deformation, leading to the self-centering capacity of the SCB does not work in reducing the displacement response. The maximum displacement of the structure is equal to its maximum vibration amplitude, so the displacement response of the BRBF is less than that of the SCBF when SMF has no residual displacement.

In general, the seismic displacement mitigation mechanism of the SCB arises from three main aspects: the enhancement of the initial stiffness of the structure; the provided additional energy dissipation; and the provided self-centering capability. The increased initial stiffness and provided additional energy dissipation capacity mainly affect the actual earthquake vibration amplitude of the structure, while the self-centering capability predominantly affects the equilibrium position of the structural vibration. Therefore, for structures without obvious residual deformation, BRB performs better for reducing the displacement responses of structure than that of the SCB, while for structures with obvious residual deformation, SCB may perform better for reducing the displacement responses of structure than that of the BRB.

5. Sensitivity Analysis Of Key Parameters Of Scb On Seismic Responses

SCB can effectively reduce the residual displacement and maximum instantaneous displacement of SMF. However, it will also simultaneously amplify the acceleration response, leading to an increase in the seismic loss of the acceleration-sensitive non-structural components. Therefore, how to design SCB according to the seismic demand of the structure and make full use of SCB is of great significance. Generally, there are four key parameters describing the mechanical properties of SCB: initial elastic stiffness K_{SCB}, post-activation stiffness coefficient α, activation strength $F_{a,SCB}$, and energy dissipation coefficient β. The larger the value of β, the more the hysteretic energy dissipated by SCB, the smaller the acceleration and displacement responses of the structure are. Under the premise of ensuring the structure returns to the initial position, the larger the β is, the more favorable the structure. Therefore, this section will only focus on the effects of the initial elastic stiffness K_{SCB}, the post-activation stiffness coefficient α, and the activation strength $F_{a,SCB}$ on the seismic responses of the structure.

5.1. Initial elastic stiffness

Based on the 8 equivalent SDOF models of SMF with different fundamental period established in Section 4.1, 9 different initial stiffnesses of the SCB are set and the other parameters of the models remain unchanged. That is, K_{SCB}/K_0 = [0.2, 0.4, 0.6, 0.8, 1.0, 1.2, 1.4, 1.6, 2.0]. Where, K_0 is the initial stiffness of SMF and K_{SCB} represents the initial stiffness of SCB system. A total of 72 equivalent SDOF models of the SCBF are thus obtained. Based on the 22 far-field ground motion records selected in this paper as the seismic input, the seismic responses of the SCBFs with different initial stiffness are obtained by 1584 NTHA. To make the results more intuitive, the seismic responses of the SCBFs are normalized by the seismic responses of the corresponding SMF. The specific normalized results are discussed below.

Normalized acceleration responses of the SCBFs are shown in Fig. 8a. All the values of normalized acceleration are greater than 1, indicating that the SCB system increases the acceleration response of the SMF. The shorter the fundamental period of the SMF, the more significantly the initial stiffness of the SCB system will increase the acceleration. For the SMF with the fundamental period of 0.2s, the SCB amplifies the acceleration by 50 ~ 69%; while for SMF with the fundamental period of 4.0s, the SCB only amplifies the acceleration by 1 ~ 2%. For SMF

with the fundamental periods of 0.2s and 0.4s, the acceleration response of SCBF increases linearly with the increase of the initial stiffness of the SCB system. For the SMF with the fundamental period equal to or greater than 0.6s, the acceleration response increases rapidly first, and then the increase rate gradually becomes slower. Moreover, for SMF with the fundamental period greater than or equal to 2s, when $K_{SCB}/K_0 \geq 1.0$, even if the initial stiffness of the SCB system continues to increase, the acceleration response of SCBF will not continue to increase.

The normalized displacement responses of SCBFs are shown in Fig. 8b. All values of normalized displacement are less than 1, indicating that the SCB system can effectively reduce the displacement response of the SMF. And the shorter the fundamental period of the SMF, the more significant the displacement reduction is achieved by SCB. For SMF with the fundamental period of 4s, the SCB reduces the structural displacement by 5%~21%, and for SMF with the fundamental period of 0.2s, the SCB reduces structural displacement by 33%~66%. As the initial stiffness of the SCB system increases, the displacement reduction effect increases gradually, but when $K_{SCB}>1.2K_0$, the rate of displacement reduction becomes increasingly stable.

The normalized residual displacement responses of SCBFs are shown in Fig. 8c. All values of the normalized residual displacement are much less than 1, indicating that the SCB system can effectively reduce the residual displacement of the SMF. And with the increase of the initial stiffness of the SCB, the residual displacement decreases gradually, but if $K_{SCB}/K_0 > 0.6$, the rate of the reduction of the residual displacement tends to be gentle.

The normalized hysteretic energy dissipated by frames of SCBF is shown in Fig. 8d. Numerous indicators are used in the damage evaluation of steel structures and energy-related damage indicators are common damage indicators (De Domenico and Hajirasouliha 2021; Rajeev and Wijesundara 2014), illustrating that the hysteretic energy of the steel structure can reflect the damage degree of the structure to a certain extent. Higher amounts of hysteresis energy indicate more serious damage of the steel structure. Figure 8d shows that with the increase of the initial stiffness of the SCB system, the hysteretic energy of the frame in SCBF decreases gradually, indicating that the damage to frames is gradually reduced. The shorter the fundamental period of the structure, the less the hysteretic energy of beams and columns of SCBF. Note that partial values of the normalized hysteretic energy in Fig. 8d are greater than 1. For example, if the fundamental period of SMF equals 4.0s and the $K_{SCB}/K_0 \leq 0.8$, the normalized hysteretic energy values are greater than 1. This means that the damage to beams and columns of SCBF is greater than the damage to beams and columns of SMF. The main function of SCB in the SCBF is to control the seismic response and reduce the damage. Therefore, in the actual design, the SCB system should be designed reasonably so that the damage of the steel frame in SCBF will not exceed the original SMF.

Overall, a rise increase in the initial stiffness of SCB will increase the acceleration response and reduce the displacement and residual displacement response of the SCBF and the damage of the steel frame. Considering acceleration, displacement, residual displacement and damage together, SCB can boost the seismic performance of SMF when $K_{SCB}/K_0 = 0.6 \sim 1.2$, and the longer the fundamental period of the steel frame, the greater the initial stiffness of the SCB should be.

5.2. Post-activation stiffness coefficient

Based on the 8 equivalent SDOF models of SMF with different fundamental period established in Section 4.1, 6 different post-activation stiffness coefficients of SCB are set and the other parameters of the models remain unchanged. That is, α=[0.01, 0.02, 0.05, 0.1, 0.2, 0.3]. A total of 48 equivalent SDOF models of SCBF are thus

obtained. Based on the 22 far-field ground motion records selected in this paper as the seismic input, the seismic responses of SCBFs with different post-activation stiffness coefficients are obtained by 1056 NTHA. The normalized seismic responses of the SCBFs are shown in Fig. 9.

Figure 9a illustrates that with the increase of the post-activation stiffness, the acceleration responses of SCBFs increase linearly, and the shorter the fundamental period, the more obvious the increase of acceleration. When the fundamental period of SMF is 0.2s, the amplification of the acceleration is between approximately 1.58 and 2.48, while if the fundamental period of SMF is 4.0s, the amplification of the acceleration is only between 1.01 and 1.05. As illustrated in Fig. 9b, the post-activation stiffness has little effect on the displacement response of the SCBF. With the increase of the post-activation stiffness, the displacement response of SCBF decreases slightly, and the longer the period, the smaller the influence. Figure 9c displays that all normalized residual displacement values are less than 0.1, indicating that the SCB can significantly reduce the residual deformation of the structure, and the residual displacement decreases slightly with the increase of the post-activation stiffness coefficient. As shown in Fig. 9d, with the increase of the post-activation stiffness coefficient, the hysteretic energy of the steel frame in SCBF increases linearly, except for the structure with the fundamental period of 0.2s. The longer the fundamental period, the more obviously the hysteresis energy increases. Therefore, in order to effectively control the damage of beams and columns, the post-activation stiffness coefficient should not be too large. For example, when the fundamental period of steel frame is 4.0s, the post-activation stiffness coefficient should not be greater than 0.05, and when the period of steel frame is 3.0s, the post-activation stiffness coefficient should not exceed 0.1.

Overall, the post-activation stiffness coefficient mainly affects acceleration response and the damage of beams and columns of the SCBF. The larger the post-activation stiffness coefficient, the larger the acceleration response, and the more serious the damage of the steel frame. And the post-activation stiffness has little effect on the displacement and residual displacement of the SCBF. Conclusively, the SCB can make the steel frame achieve a better performance when the value of the post-activation stiffness coefficient does not exceed 0.1.

5.3. Activation strength

Based on the 8 equivalent SDOF models of SMF with different fundamental period established in Section 4.1, 9 different activation strength of SCBs are set and the other parameters of the models remain unchanged. That is, $F_{a,SCB}/F_y$=[0.2, 0.4, 0.6, 0.8, 1.0, 1.2, 1.4, 1.6, 1.8]. Where, F_y is the yield strength of SMF and $F_{a,SCB}$ represents the activation strength of SCB. A total of 72 equivalent SDOF models of the SCBFs are thus obtained. Based on the 22 far-field ground motions selected in this paper as the seismic input, the seismic responses of the SCBFs with different $F_{a,SCB}$ are obtained by 1584 NTHA. And the normalized seismic responses of the SCBFs are displayed in Fig. 10.

As illustrated in Fig. 10a, $F_{a,SCB}$ has a significant effect on the acceleration response of the SCBF. As $F_{a,SCB}$ increases, the acceleration response of the SCBF increases linearly. The shorter the fundamental period of the steel frame, the more significant the influence of the activation strength on the acceleration. When the fundamental period of the steel frame is 4.0s, the maximum magnification of acceleration is only about 1.04, and when the fundamental period is 0.2s, the magnification of acceleration reaches a range of 1.26 ~ 1.97. The greater the acceleration response of the structure, the larger the seismic loss of the acceleration-sensitive non-structural components. Therefore, from the perspective of controlling the acceleration, the activation strength of the SCB system should not be too high. Figure 10b displays that as the activation strength of the SCB increases,

the displacement response of SCBF decreases rapidly, and the shorter the fundamental period of the steel frame, the more significant the influence of activation strength on displacement. When the fundamental period of the steel frame is 4.0s, the displacement response of SCBF is reduced by 12%~21%, and when the fundamental period of the steel frame is 0.2s, the displacement response of the SCBF is reduced by 31%~70%. Therefore, from the perspective of controlling the displacement response, the greater the activation strength of the SCB, the smaller the structural displacement response. Figure 10c shows that $F_{a,SCB}$ has a significant effect on the residual displacement of the SCBF. With the increase of the activation strength, the residual displacement of the SCBF decreases rapidly. And when $F_{a,SCB}/F_y$ >0.8, the rate of decrease of the residual displacement gradually becomes gentle. Figure 10d indicates that when the fundamental period of the steel frame does not exceed 0.4 s, the damage of the steel frame in the SCBF gradually decreases with the increase of the activation strength, and all the damage of the steel frames is reduced compared to the damage of the original SMF. When the fundamental period of the steel frame is more than 0.4s, the damage of the steel frame decreases first and then rises with the increase of the activation strength. Particularly for the long-period structure, the damage of the steel frame even exceeds the damage of the original SMF. For example, when $F_{a,SCB}/F_y$ >1.2 at the fundamental period of 4.0 s, the values of the normalized hysteresis energy of the steel frame in the SCBF exceed 1, indicating that the damage of the steel frame exceeds the damage of the corresponding SMF.

Overall, the activation strength has a significant effect on the acceleration, displacement, residual displacement of the SCBF and the damage of steel frame. As $F_{a,SCB}$ increases, the acceleration response increases gradually, and the displacement and residual displacement response gradually decrease. For short-period structures, the damage of the steel frame is gradually reduced, while for the medium- or long-period structures, the damage of the steel frame is first reduced and then increased. It can be concluded that, the SCB can enhance the seismic performance of the SMF when $F_{a,SCB}/F_y$ = 0.6 ~ 1.2.

6. Conclusions

SCB is an efficient component to reduce residual displacement and improve the seismic resilience of steel frames. Based on the equivalent SDOF model, the NTHA is adopted to study the seismic displacement mitigation mechanism of SCBF. The influence of key parameters of SCB such as initial stiffness, post-activation stiffness coefficient and activation strength on the seismic performance of SCBF was also discussed. And reasonable value ranges for the key parameters were suggested. The following general conclusions have been drawn:

1. The SCB can not only successfully reduce the residual displacement of the structure, but also reduce the maximum displacement response. The mechanism of displacement reduction includes three main aspects: the enhancement of the initial stiffness of the structure; the provided additional hysteretic energy dissipation; and the provided self-centering capability. The increased initial stiffness and provided additional hysteretic energy mainly affect the actual earthquake vibration amplitude of the structure, while the self-centering capability predominantly influences the equilibrium position of the structural vibration.

2. The initial stiffness of SCB has a significant effect on the acceleration, displacement and residual displacement of the SCBF, as well as the damage of the steel frame. The larger the initial stiffness, the larger the acceleration response of SCBF, and the smaller the displacement, residual displacement and the damage of the steel frame. The SCB can enhance the seismic performance of SMF when K_{SCB}/K_0 = 0.6 ~ 1.2.

3. The post-activation stiffness coefficient of SCB mainly affects the acceleration response of the SCBF and the damage of the frame. The larger the post-activation stiffness coefficient, the larger the acceleration response, and the more serious the damage of the steel frame. Therefore, the value of the post-activation stiffness coefficient has better not exceed 0.1.
4. The $F_{a,SCB}$ has a significant effect on the acceleration, displacement, and residual displacement of the SCBF, as well as the damage of the steel frame. The greater the $F_{a,SCB}$, the larger the acceleration response of SCBF, and the smaller the displacement and residual displacement. A good seismic performance can be achieved when $F_{a,SCB}/F_y = 0.6 \sim 1.2$.

Declarations

Funding

This work was supported by the National Natural Science Foundation of China (Grant No. 52125804 and 52078036).

Competing Interests

The authors have no relevant financial or non-financial interests to disclose.

Author Contributions

All authors contributed to the study conception and design. Material preparation, data collection and analysis were performed by Xiao Lu. The first draft of the manuscript was written by Xiao Lu and all authors commented on previous versions of the manuscript. All authors read and approved the final manuscript.

References

1. Christopoulos C, Filiatrault A, Folz B. (2002) Seismic response of self-centring hysteretic SDOF systems. Earthq Eng Struct D 31(5): 1131–1150. https://doi.org/10.1002/eqe.152
2. Christopoulos C, Tremblay R, Kim HJ, Lacerte M. Self-centering energy dissipative bracing system for the seismic resistance of structures: development and validation, J Struct Eng 2008; 134 (1): 96–107. https://doi.org/10.1061/(ASCE)0733-9445(2008)134:1(96)
3. De Domenico D, Hajirasouliha I. (2021) Multi-level performance-based design optimization of steel frames with nonlinear viscous dampers. B Earthq Eng 19(12): 5015–5049. https://doi.org/10.1007/s10518-021-01152-7
4. Erochko J, Christopoulos C, Tremblay R, Choi H. (2011) Residual drift response of SMRFs and BRB frames in steel buildings designed according to ASCE 7 − 05. J Struct Eng 137(5): 589–599. https://doi.org/10.1061/(ASCE)ST.1943-541X.0000296
5. FEMA-P695 (2009) Quantification of building seismic performance factors. Washington; 2009.
6. Lin ZC, Xu LH, Xie XS. (2022) Development and seismic performance improvement of hybrid damping self-centering braced frame. J Build Eng 104388. https://doi.org/10.1016 /j.jobe.2022.104388
7. McCormick J, Aburano H, Ikenaga M, et al. (2008) Permissible residual deformation levels for building structures considering both safety and human elements. In: Proceedings of the 14th world conference on

earthquake engineering. Beijing.

8. Miller DJ. (2012) Development and experimental validation of a nickel-titanium shape memory alloy self-centering buckling-restrained brace. Eng Struct 40: 288–298. https://doi.org/10.1016/ j.engstruct.2012.02.037
9. Pirooz R M, Habashi S, Massumi A. (2021) Required time gap between mainshock and aftershock for dynamic analysis of structures. B Earthq Eng 19(6): 2643–2670. https://doi.org/10.1007/ s10518-021-01087-z
10. Rajeev P, Wijesundara K K. (2014) Energy-based damage index for concentrically braced steel structure using continuous wavelet transform. J Constr Steel Res 103: 241–250. https://doi.org/10.1016/j.jcsr.2014.09.011
11. Tremblay R, Lacerte ; M, Christopoulos C. (2008) Seismic response of multistory buildings with self-centering energy dissipative steel braces. J Struct Eng 134(1): 108–120. https://doi.org/10.1061/(ASCE)0733-9445(2008)134:1(108)
12. Velasco L, Hospitaler A, Guerrero H. (2022) Optimal design of the seismic retrofitting of reinforced concrete framed structures using BRBs. B Earthq Eng https://doi.org/10.1007/s10518-022-01394-z
13. Wang H, Nie X, Pan P. (2017) Development of a self-centering buckling restrained brace using cross-anchored pre-stressed steel strands. J Constr Steel Res 138: 621–632. https://doi.org/10.1016/j.jcsr.2017.07.017
14. Xiao S, Xu L, Li Z. (2019) Seismic performance and damage analysis of RC frame–core tube building with self-centering braces. Soil Dyn Earthq Eng 120: 146–157. https://doi.org/10.1016/j.soildyn.2019.01.029
15. Xu LH, Fan XW, Li ZX. (2017a) Cyclic behavior and failure mechanism of self-centering energy dissipation braces with pre-pressed combination disc springs. Earthq Eng Struct D 46(7): 1065–1080. https://doi.org/10.1002/eqe.2844
16. Xu LH, Fan XW, Li ZX. (2017b) Hysteretic analysis model for pre-pressed spring self-centering energy dissipation braces. J Constr Steel Res 139: 363–373. https://doi.org/10.1061/(ASCE)ST.1943-541X.0002060
17. Xu LH, Lin ZC, Xie XS. (2022) Assembled self-centering energy dissipation braces and a force method-based model. J Constr Steel Res 190: 107121. https://doi.org/10.1016/ j.jcsr.2021.107121
18. Zarrin M, Daei A, Heydary T. (2021) A simplified normalized multi-mode nonlinear static procedure (NMP) for seismic performance evaluation of building structures. B Earthq Eng 19(13): 5711–5741. https://doi.org/10.1007/s10518-021-01185-y
19. Zhou Y, Song G, Tan P. (2019) Hysteretic energy demand for self-centering SDOF systems. Soil Dyn Earthq Eng 125: 105703. https://doi.org/10.1016/j.soildyn.2019.105703
20. Zhu S, Zhang Y. (2008) Seismic analysis of concentrically braced frame systems with self-centering friction damping braces. J Struct Eng 134: 121–131. https://doi.org/10.1061/(ASCE)0733-9445(2008)134:1(121)

Figures

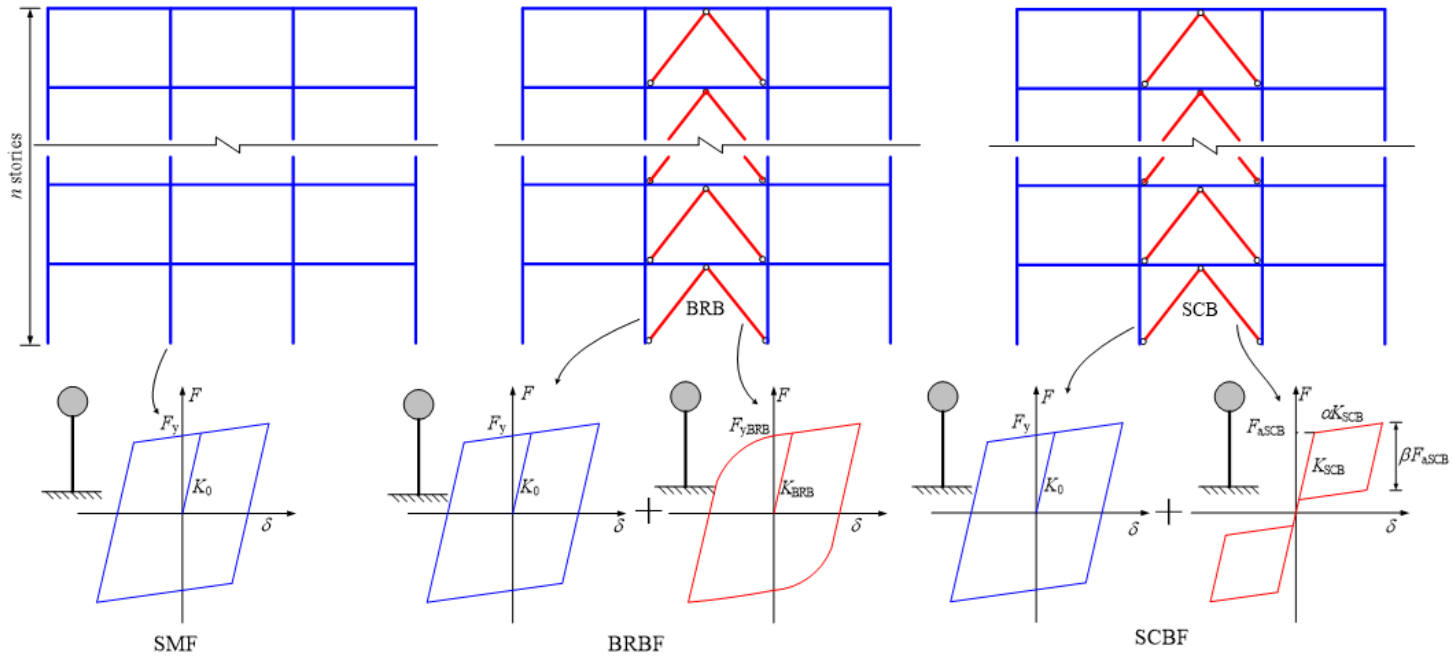

Figure 1

Schematic diagram of hysteresis models for SMF, BRBF and SCBF

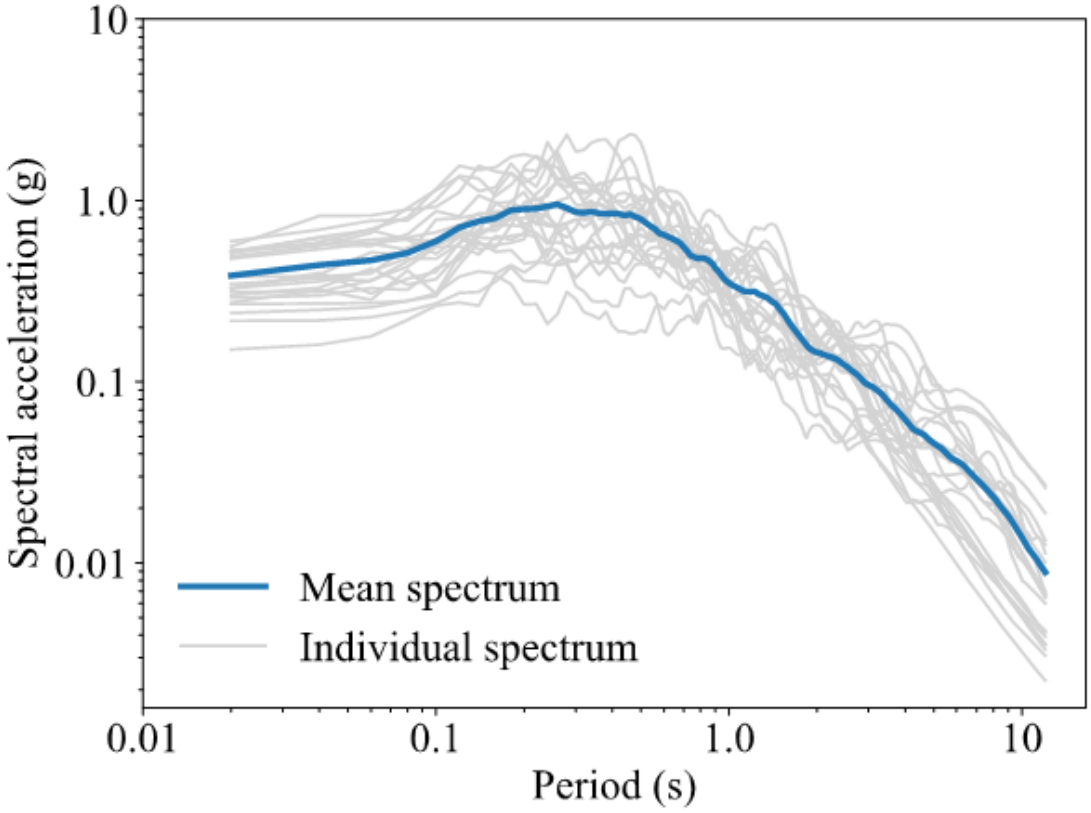

Figure 2

Response spectra of 22 individual normalized far-field ground motion records and the mean spectrum of the total records

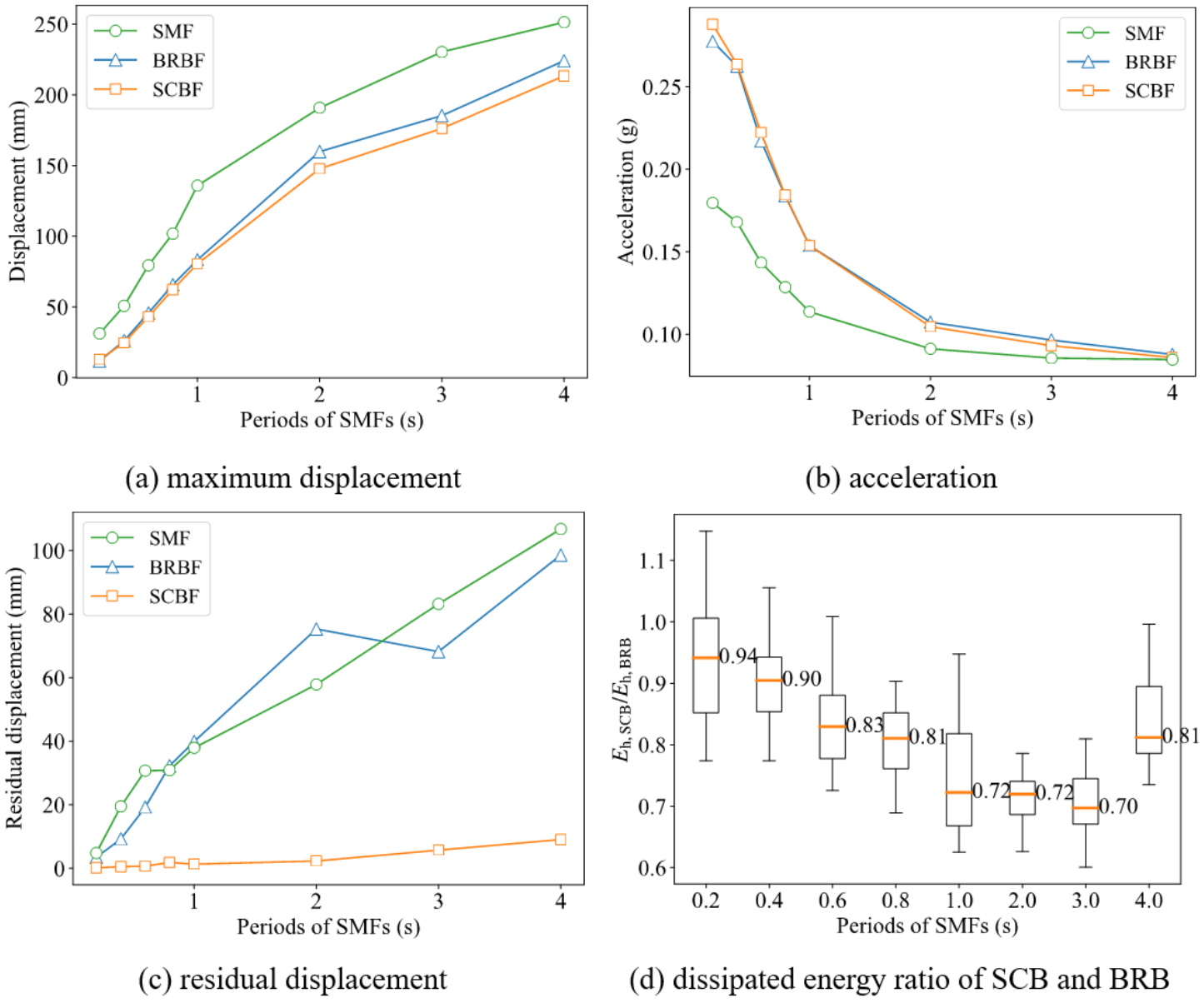

Figure 3

Structural seismic responses of SMFs, BRBFs and SCBFs with different periods

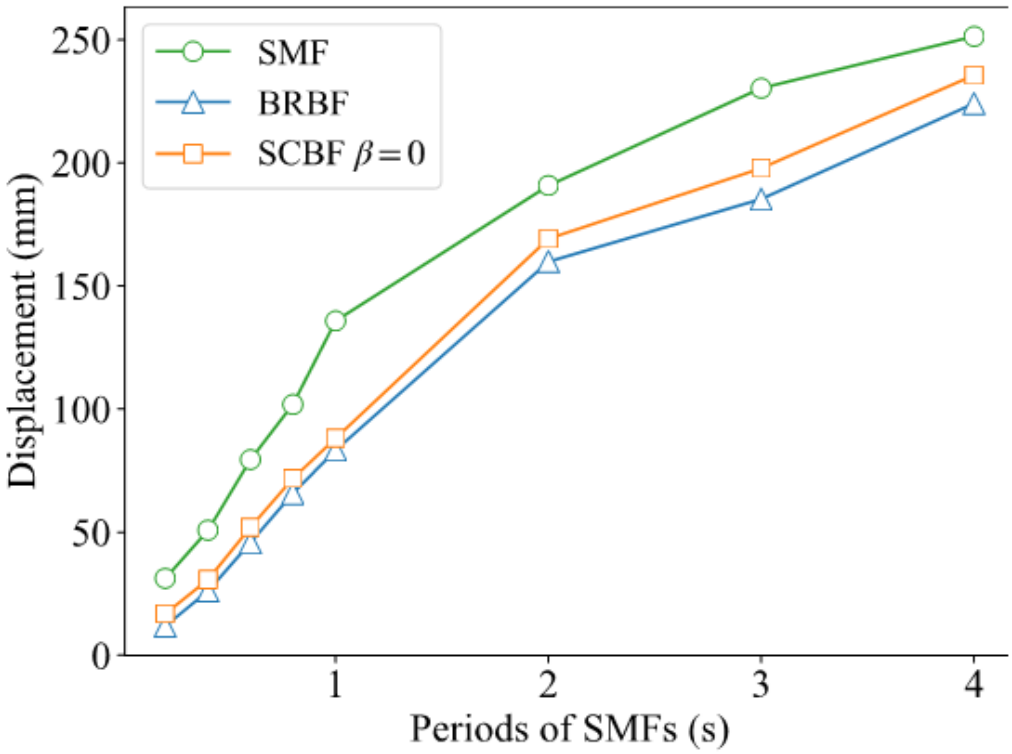

Figure 4

Displacement responses of SCBFs with β=0

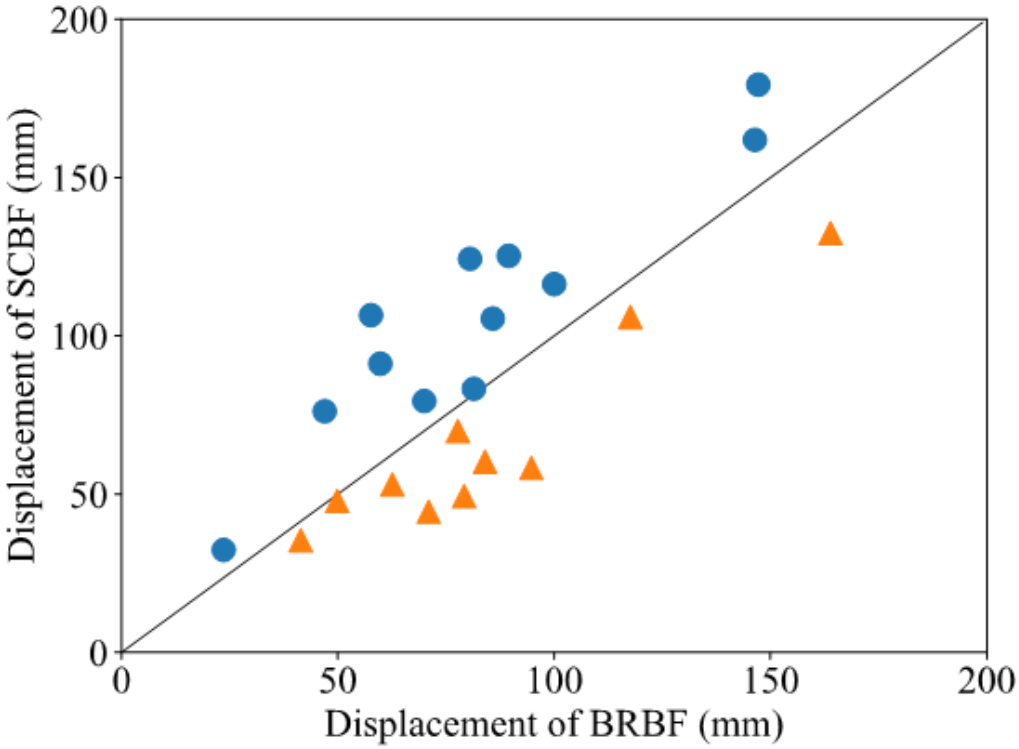

Figure 5

Comparation of displacement responses between BRBF and SCBF under 22 ground motion records

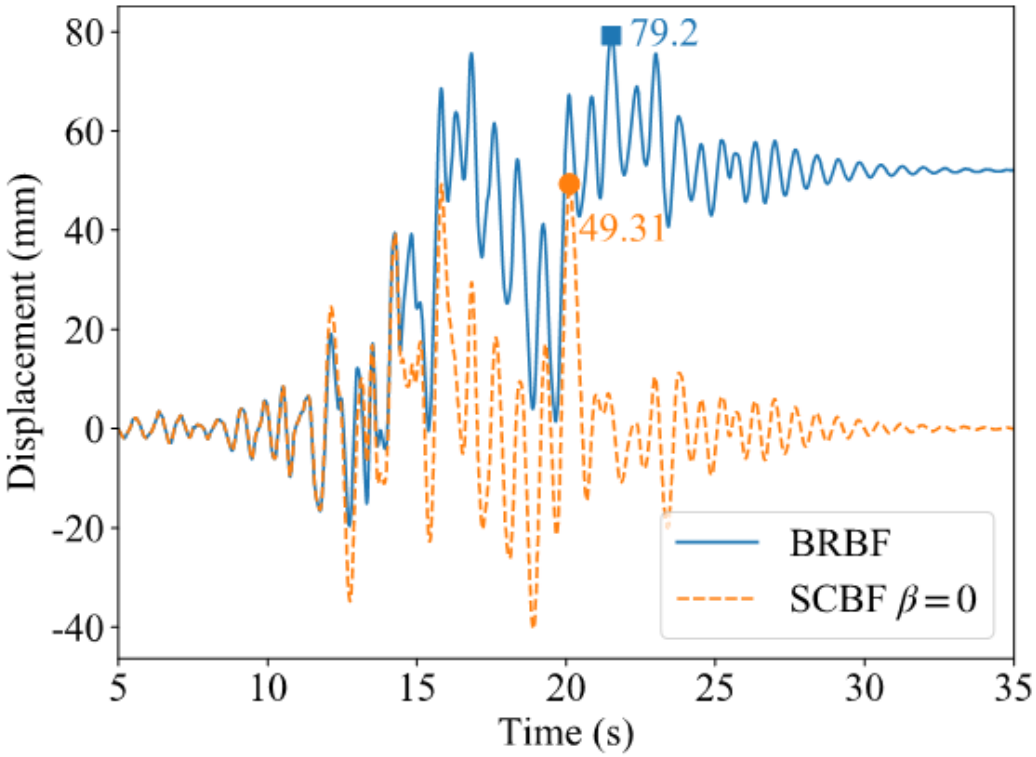

Figure 6

Displacement time history of the BRBF and the SCBF under the ground motion of LANDERS_CLW-LN

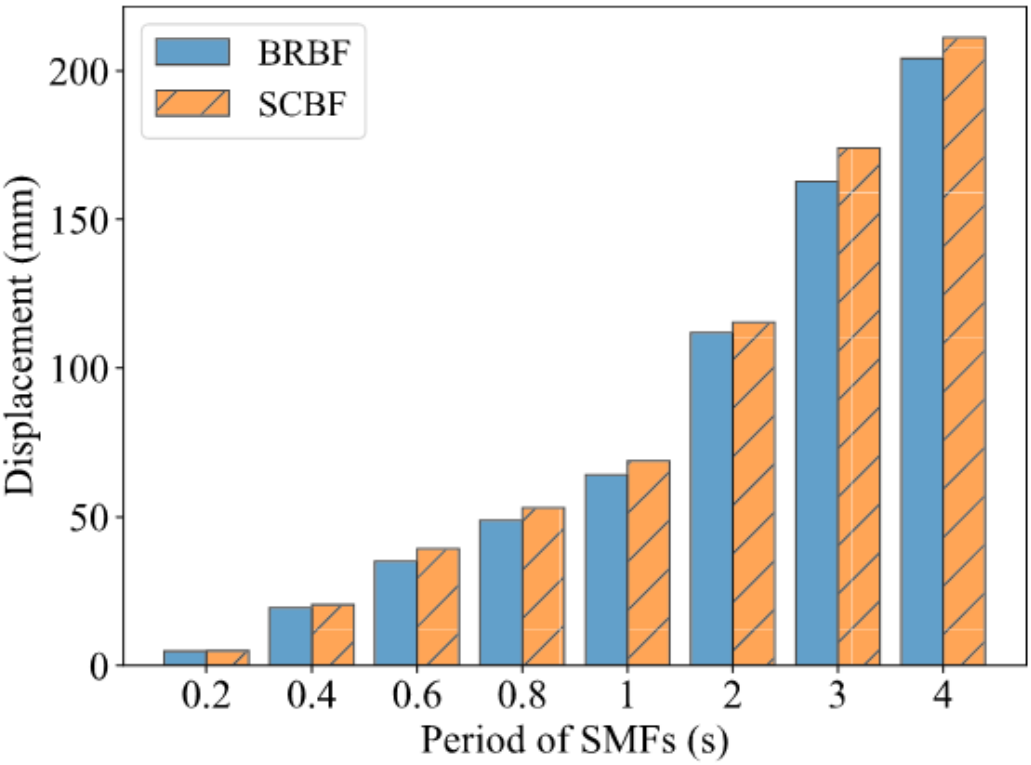

Figure 7

Displacement of SCBF and BRBF without residual displacement

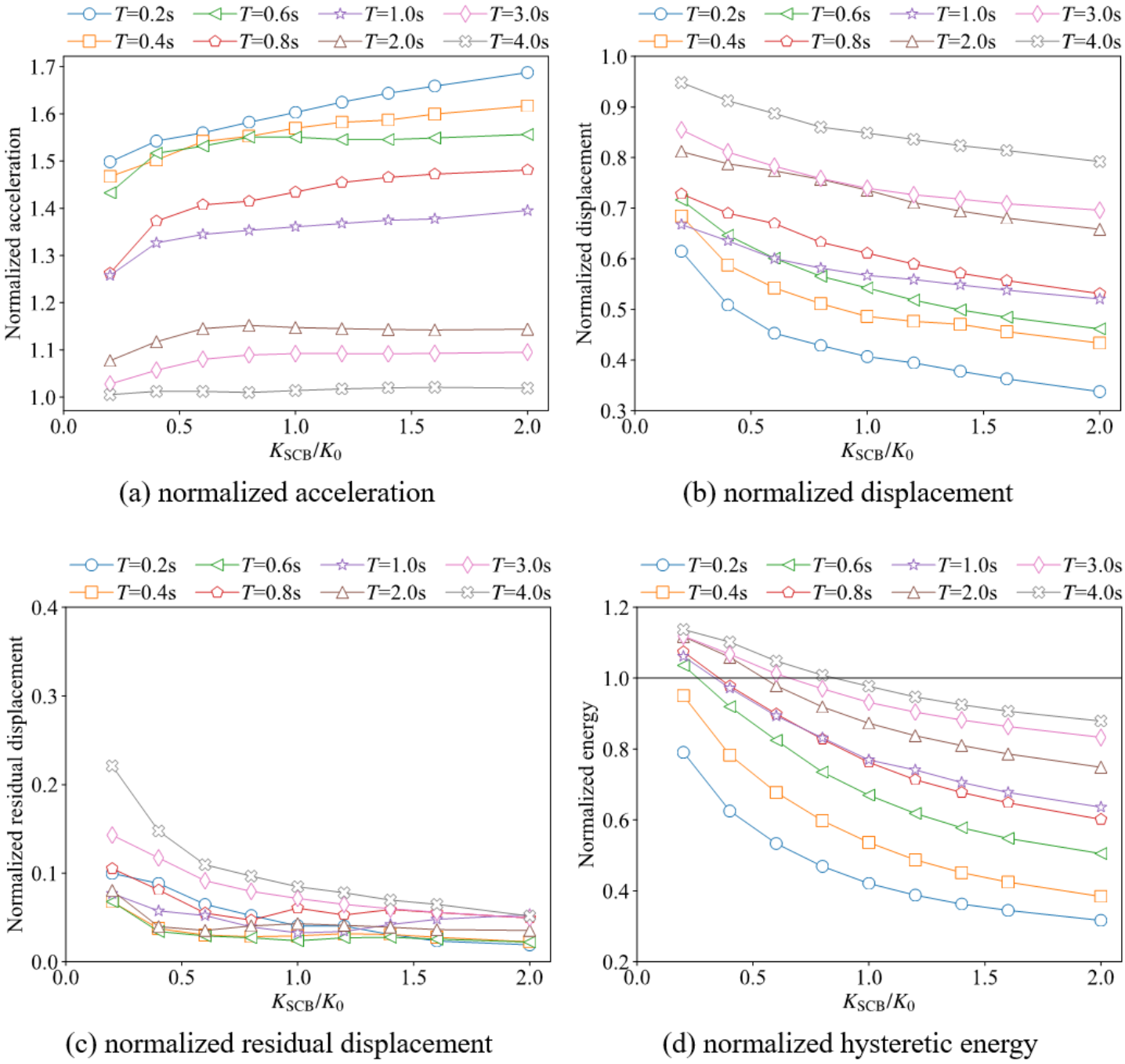

Figure 8

Seismic responses of SCBF with different initial stiffness of SCB

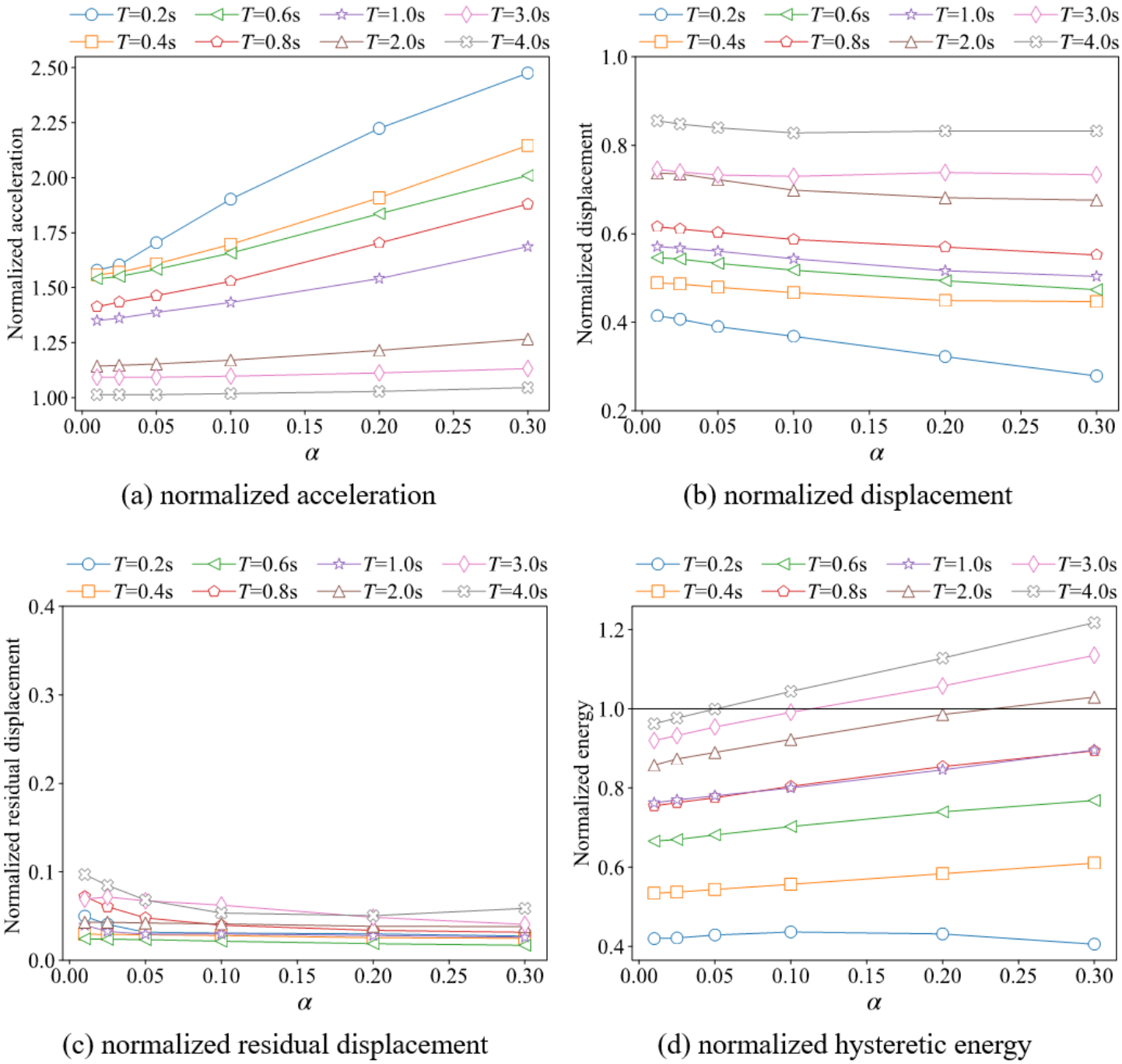

Figure 9

Seismic responses of SCBF with different post-activation stiffness of SCB

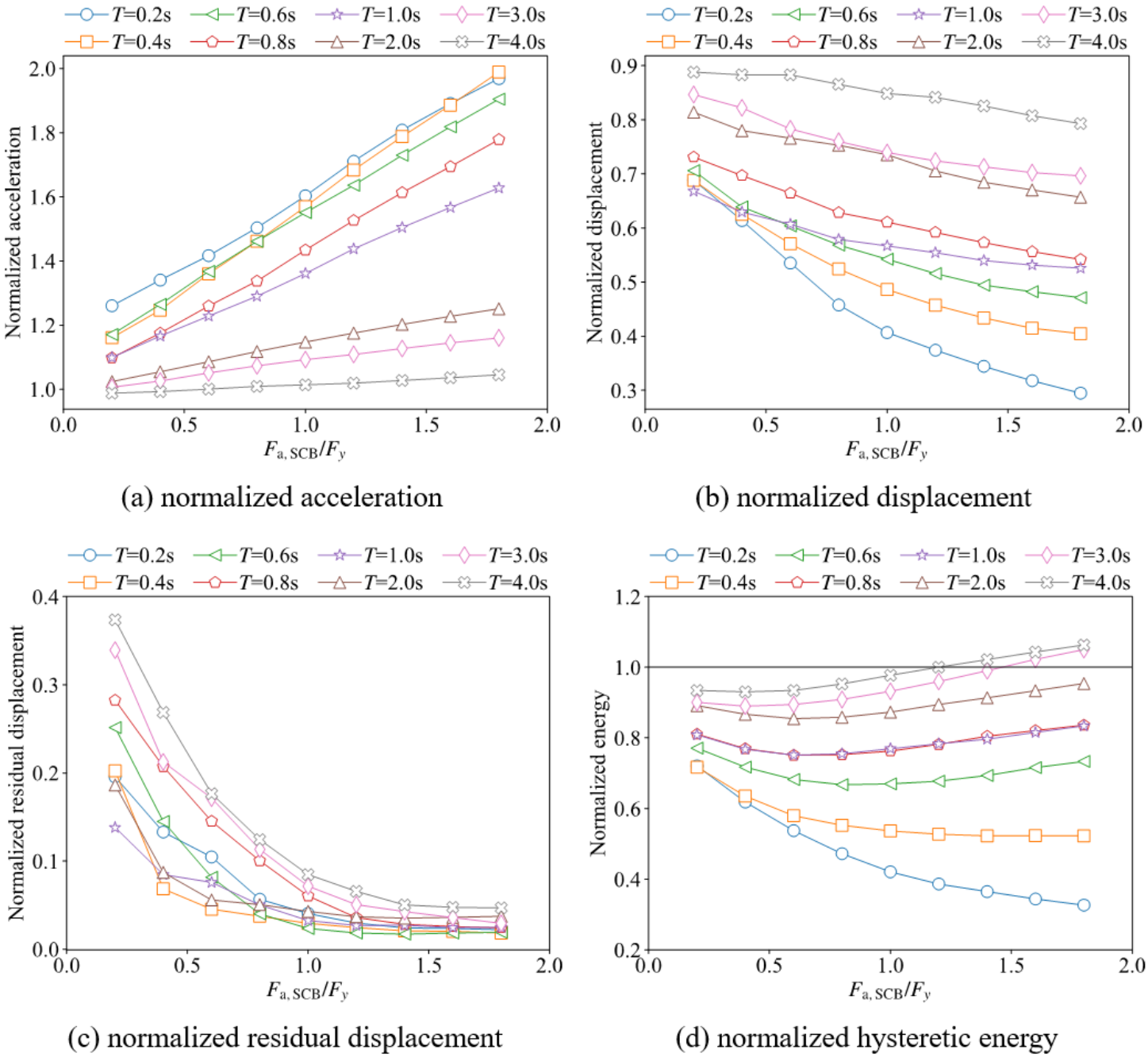

Figure 10

Seismic responses of SCBF with different $F_{a,SCB}$